The present thesis entitled "**Isolation, purification and characterization of polysaccharide and their use in the synthesis of metal nanoparticles and study of biological activities**" is divided into five chapters.

CHAPTER-I: This chapter is subdivided into two parts.

PART A: This part of chapter-I describes the introduction of carbohydrates, polysaccharides, especially mushroom polysaccharides on which the present investigation was carried out and some of their important biological activities. Carbohydrates are essential constituents of all living organisms and have a variety of vital functions. According to Robyt "Carbohydrates are polyhydroxy aldehydes or ketones or compounds that can be derived from them by oxidation, reduction or replacement of different functional groups." These are generally classified into four classes: monosaccharides, disaccharides, oligosaccharides, and polysaccharides. The great bulk of the carbohydrates in nature are present as polysaccharides, which are very large and complex molecules. Almost all living organism like fungi, plant etc. produces polysaccharides which are made up of chains of monosaccharides (the sugars) and linked together by glycosidic bonds. According to their structural features, polysaccharides can be classified as- (1) homopolysaccharides which are composed of one type of monosaccharides e.g. starch, cellulose, dextran etc. and (2) heteropolysaccharides which are composed of different monosaccharide units e.g. mannogalactan, xyloglucan, glucomannan etc.

Since the last few decades, polysaccharides from mushroom have drawn the attention of chemist and immunobiologists due to their immunomodulatory and antitumor properties. The main active components of the mushroom polysaccharides were proved to be the glucans, specifically β-D-glucans which are important for their outstanding ability to enhance and stimulate the immune systems and are thus regarded as typical biological response modifiers (BRMs). They possess antitumor effect through host defence mechanism against tumor without side effect. Except for β-D-glucans several polysaccharides having different composition and structure also showed biological effects. Currently, several mushroom polysaccharides isolated from *Lentinus edodes*, *Schizophyllum commune*, *Agaricus blazei*, *Grifola Frondosa*, and *Ganoderma lucidum* are widely used clinically as anti-tumor agents and many of them have been commercialized throughout the world. The biological activities of polysaccharides depend on the

molecular structure, molecular weight, size, branching frequency, structural modification, conformation, and solubility. It is therefore important to determine the exact structure and biological activity of the polysaccharides isolated from mushrooms.

PART B: This part deals with the discussion about synthesis of metal nanoparticles, especially gold nanoparticles via green route and various applications of nanoparticles in different fields. Utilization of nontoxic chemicals, environmentally benign solvents and renewable materials are some of the key issues for green synthesis strategy of metal nanoparticles. In recent years, biomolecules such as polysaccharides from plant and mushrooms are used in the synthesis of gold nanomaterials. In this route, biomolecules serve both as reducing and stabilizing agent. Microorganisms are also used for the synthesis of gold nanoparticles. Among the various applications of metal nanoparticles, the role of metal nanoparticles in the field of catalysis opens a new horizon. Metal nanoparticles in particular gold nanoparticles serve as an effective catalyst in the reduction of various pollutants like 4-NP, the most common organic pollutant in industrial and agricultural waste water. Green synthesis of metal nanoparticles and role of metal nanoparticles in the field of catalysis have been illustrated in this part.

CHAPTER-II: This chapter is also subdivided into two parts.

PART A: The methodologies that have been adopted during the whole course of the research tenure to determine the structure of polysaccharides and immunomodulating studies have been discussed in this part. The immunomodulating properties of the polysaccharides depend on the size of molecule, branching rate and form. So, it is very important to determine the exact structure of the polysaccharides. Purification of the polysaccharides should be done carefully as slight contamination of foreign sugar leads to wrong interpretation of the structure. The polysaccharide was purified using chromatographic technique like gel permeation chromatography. The accurate structures of the polysaccharides were determined using two types of methods:

(1) Chemical methods that include acid hydrolysis, methylation, and periodate oxidation studies.
(2) Spectroscopic method comprising of 1D (^{1}H, ^{13}C, and DEPT-135) and 2D NMR (DQF-COSY, TOCSY, NOESY, ROESY, HSQC, and HMBC).

The immunomodulating properties of different polysaccharides were examined by NO production by macrophages using Griess reagent. The activation of splenocyte and thymocyte tests were carried out in mouse cell culture medium with polysaccharide by the MTT [3-(4,5-dimethylthiazol-2-yl)-2,5-diphenyltetrazolium bromide] method.

PART B: In this part the detailed procedure of the synthesis of the gold nanoparticles (Au NPs) and the various techniques used in the characterization of the Au NPs have been discussed. The Au NPs were synthesized using gum polysaccharide of *Cochlospermum religiosum* (Katira gum) which acts as both reducing and stabilizing agent. The synthesized Au NPs were characterized using UV-vis, HR-TEM, XRD, and FT-IR techniques. The reduction of 4-NP to 4-AP by $NaBH_4$ in aqueous phase was studied as a model reaction to prove the catalytic activity of synthesized Au NPs.

CHAPTER-III: This chapter covers the isolation, purification, structural characterization and immunomodulating properties of a polysaccharide (PS) isolated from the edible hybrid mushroom *pfle 1q*, obtained through intergeneric protoplast fusion between *Pleurotus florida* and *Lentinula edodes*. Aqueous extract of fruit bodies of the hybrid mushroom strain, *pfle 1q* yielded single polysaccharide fraction, named as PS.

Structural analysis of PS

The PS showed a specific rotation of $[\infty]_D^{30.9}$ + 50.08 (*c* 0.09, water). The apparent average molecular weight of the PS fraction was estimated as 1.55×10^5 Da. The GLC analysis of the alditol acetates of the hydrolyzed product of PS confirmed the presence of mannose and galactose in a molar ratio of nearly 1:2. The absolute configuration of the monosaccharides was determined as D. The GLC-MS analysis of partially methylated alditol acetates revealed the presence of 1,5-di-*O*-acetyl-2,3,4,6-tetra-*O*-methyl-D-mannitol, 1,5,6-tri-*O*-acetyl-2,3,4-tri-*O*-methyl-D-galactitol, 1,2,5,6-tetra-*O*-acetyl-3,4-di-*O*-methyl-D-galactitol in a molar ratio of nearly 1:1:1. Thus, PS was assumed to consist of terminal D-mannopyranosyl, (1→6)-linked D-galactopyranosyl, and (1→2,6)-linked D-galactopyranosyl moieties respectively. These linkages were further confirmed by periodate oxidation experiment. The GLC-MS analysis of the alditol acetates of periodate oxidized, reduced, methylated PS showed total disappearance of sugar residues. These results indicated that all the sugar residues were consumed during oxidation. Thus, the mode of linkages present in the PS was confirmed.

The ^{1}H NMR spectrum of PS showed the presence of three signals in the anomeric region at δ 5.14, 5.00 and 4.81 in a ratio of nearly 1:1:1. They were designated **A**, **B**, and **C** according to their decreasing proton chemical shifts. Three signals in the anomeric region of ^{13}C spectrum at δ 101.6, 98.3, and 97.8 correlated to the residues **C**, **A**, and **B** respectively from HSQC spectrum. The rest of the ^{1}H and ^{13}C signals were assigned from DQF-COSY, TOCSY, and HSQC experiments. The proton coupling constants were measured from DQF-COSY experiment.

On the basis of proton and carbon chemical shifts, proton-proton coupling constants, and C-1, H-1 coupling constants, all the sugar residues were assigned as follows:

Residue **A:** (1→2,6)-linked α-D-galactopyranosyl residue.

Residue **B:** (1→6)-linked α-D-galactopyranosyl residue

Residue **C:** terminal β-D-mannopyranosyl residue

The different linkages that connected these three residues were determined from ROESY as well as NOESY spectrum. In ROESY spectrum, the inter-residual connectivities were observed between **A**H-1/**B**H-6a and **B**H-6b, **B**H-1/**A**H-6a and **A**H-6b, and **C**H-1/**A**H-2 along with other intra-residual contacts. Thus, from ROESY spectrum the following linkages were established.

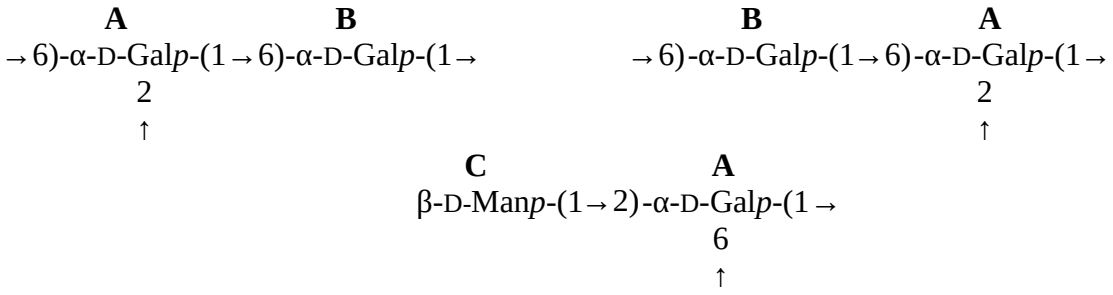

These connectivities were further confirmed from HMBC experiment. In HMBC spectrum the inter-residual cross-peaks were observed between **A**H-1/**B**C-6, **A**C-1/**B**H-6a and **B**H-6b, **B**H-1/**A**C-6, **B**C-1/**A**H-6a and **A**H-6b, **C**H-1/**A**C-2, and **C**C-1/**A**H-2. Thus, the HMBC and ROESY connectivities clearly supported the presence of the following repeating unit in the PS:

A **B**

→6)-α-D-Gal*p*-(1→6)-α-D-Gal*p*-(1→

2

↑

1

β-D-Man*p*

C

Immunomodulating properties of PS

Mushroom polysaccharides function as immunostimulator by activating the macrophages. Macrophages are white blood cells which play key roles in immune system defense. They usually engulf and destroy bacteria and viruses. Hence, macrophage activation induced by the PS was tested *in vitro*. On treatment with different concentrations of this PS it was observed that 25% to 34% of NO production increased up to 25 µg/mL. This was further increased by 87% to 114% at 50 and 100 µg/mL respectively, but decreased at 200 µg/mL. Hence, an enhanced production of NO i,e. the effective dose of this PS was observed at 100 µg/mL with optimum production of 12.8 µM NO per 5×10^5 macrophages.

Proliferation of splenocyte and thymocyte is an indicator of immunostimulation. The splenocyte and thymocyte activation tests were carried out in mouse cell culture medium with the PS by the MTT [3-(4,5-dimethylthiazol-2-yl)-2,5-diphenyltetrazolium bromide] method. The splenocyte and thymocyte proliferation indices as compared to PBS control if closer to 100 or below indicate low stimulatory effect on immune system. Both the splenocyte and thymocyte proliferation indices were found maximum at 50 µg/mL, above and below which it decreases. Hence, it can be concluded that 50 µg/mL is the optimum concentration of the PS for splenocyte and thymocyte proliferation.

CHAPTER-IV: This chapter describes the isolation, purification, and structural characterization and immunomodulating properties of a polysaccharide (PS-I) isolated from the edible hybrid mushroom *pfle 1p* obtained through intergeneric protoplast fusion between *Pleurotus florida* and *Lentinula edodes*. Aqueous extract of fruit bodies of the hybrid mushroom strain, *pfle 1p* yielded two polysaccharide fractions named as PS-I and PS-II.

Structural analysis of PS-I

The PS-I showed specific rotation $[\alpha]_D^{29.2}$ +32.6 (*c* 0.886, water). The average molecular weight of PS-I was estimated as ~2.1×10^5 Da from a calibration curve prepared with

standard dextrans. GLC analysis of alditol acetates of hydrolyzed product of PS-I confirmed the presence of glucose, galactose, and mannose almost in a ratio of 4:2:1. The absolute configuration of the sugar residues were determined as D. The GLC-MS analysis of partially methylated alditol acetates of PS-I revealed the presence of seven peaks in a molar ratio of nearly 1:1:1:1:1:1:1. The peaks were assigned as

1,5-di-*O*-acetyl-2,3,4,6-tetra-*O*-methyl-D-glucitol
1,5-di-*O*-acetyl-2,3,4,6-tetra-*O*-methyl-D-mannitol
1,5,6-tri-*O*-acetyl-2,3,4-tri-*O*-methyl-D-galactitol
1,5,6-tri-*O*-acetyl-2,3,4-tri-*O*-methyl-D-glucitol
1,3,5-tri-*O*-acetyl-2,4,6-tri-*O*-methyl-D-glucitol
1,3,4,5-tetra-*O*-acetyl-2,6-di-*O*-methyl-D-glucitol
1,2,5,6-tetra-*O*-acetyl-3,4-di-*O*-methyl-D-galactitol

Thus, PS-I was assumed to be consist of terminal D-glucopyranosyl, and D-mannopyranosyl, (1→6)-linked D-galactopyranosyl, (1→6)-linked D-glucopyranosyl, (1→3)-linked D-glucopyranosyl, (1→3,4)-linked D-glucopyranosyl, and (1→2,6)-linked D-galactopyranosyl moieties, respectively. These linkages were further confirmed by periodate oxidation experiment. The GLC-MS analysis of the alditol acetates of periodate oxidized, reduced and methylated PS-I showed the presence of 1,3,4,5-tetra-*O*-acetyl-2,6-di-*O*-methyl-D-glucitol and 1,3,5-tri-*O*-acetyl-2,4,6-tri-*O*-methyl-D-glucitol in a molar ratio of nearly 1:1. These results clearly indicated that the all other moieties except (1→3,4)-linked D-glucopyranosyl and (1→3)-linked D-glucopyranosyl were consumed during oxidation. Thus, the mode of linkages present in the PS-I were confirmed.

The ^{1}H NMR spectrum showed seven peaks in the anomeric region. The peaks were observed at δ 5.35, 5.12, 4.98, 4.78, 4.75, 4.51, and 4.49 in a ratio of nearly 1:1:1:1:1:1:1. They were designated as **A**, **B**, **C**, **D**, **E**, **F**, and **G** according to their decreasing proton chemical shifts. Seven peaks in the anomeric region of ^{13}C spectrum at δ 97.8, 98.2, 99.7 101.7, 102.4, 102.5, and 102.8 correlated to the residues **C**, **B**, **A**, **D**, **E**, **F**, and **G**, respectively from the HSQC spectrum. All the ^{1}H and ^{13}C signals were assigned using DQF-COSY, TOCSY, and HSQC experiments. The proton coupling constants were measured from DQF-COSY experiment.

On the basis of proton and carbon chemical shifts, proton-proton coupling constants, and C-1, H-1 coupling constants, all the sugar residues were assigned as follows:

Residue **A:** (1→6)-linked α-D-glucopyranosyl residue

Residue **B:** (1→2,6)-linked α-D-galactopyranosyl residue

Residue **C:** (1→6)-linked α-D-galactopyranosyl residue

Residue **D:** terminal β-D-mannopyranosyl residue

Residue **E:** (1→3)-linked β-D-glucopyranosyl residue

Residue **F:** (1→3,4)-linked β-D-glucopyranosyl residue

Residue **G:** terminal β-D-glucopyranosyl residue

The different linkages that connected these seven residues were determined from NOESY as well as ROESY spectrum. In NOESY spectrum, the inter-residual connectivities were observed between **A**H-1/**B**H-6a; **A**H-1/**B**H-6b; **B**H-1/**C**H-6a; **B**H-1/**C**H-6b; **C**H-1/**E**H-3; **D**H-1/**B**H-2; **E**H-1/**F**H-3; **F**H-1/**A**H-6a; **F**H-1/**A**H-6b; **G**H-1/**F**H-4 along with other intra-residual contacts. Finally, these connectivities were confirmed from HMBC spectrum. In this spectrum the inter-residual cross-peaks were observed between **A**H-1/**B**C-6; **A**C-1/**B**H-6a and **B**H-6b; **B**H-1/**C**C-6; **B**C-1/**C**H-6a and **C**H-6b; **C**H-1/**E**C-3; **C**C-1/**E**H-3; **D**H-1/**B**C-2; **D**C-1/**B**H-2; **E**H-1/**F**C-3; **E**C-1/**F**H-3; **F**H-1/**A**C-6; **F**C-1/**A**H-6a and **A**H-6b; **G**H-1/**F**C-4; and **G**C-1/**F**H-4. Thus, the probable structural motif present in PS-I was established as:

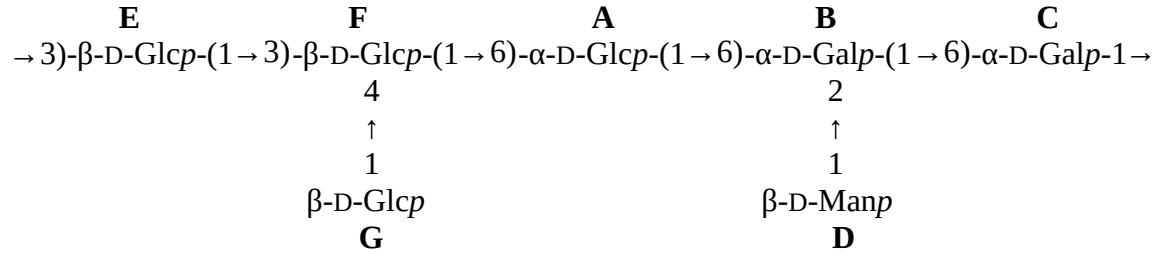

Immunomodulating properties of PS-I

To test immunomodulatory effects of PS-I, murine macrophages were incubated with PS-I in a humidified atmosphere of 5% CO_2 at 37 °C for 48 h and the production of nitric oxide (NO) was measured using Griess reagent (1:1 of 0.1% in 1-napthylethylenediamine in 5% phosphoric acid and 1% sulfanilamide in 5% phosphoric acid). On treatment with different concentrations of the PS-I, it was observed that NO production increased with increase in concentration up to 50 µg/mL with optimum production of 19.27 µM NO per 5×10^5

macrophages at 50 µg/mL which subsequently decreased with increase in concentration. Hence, the effective dose of the PS-I for macrophage activation was 50 µg/mL. Splenocyte is the cells present in the spleen that include T cells, B cells, dendritic cells, etc. that stimulate the immune response in living organism whereas thymocyte is the hematopoietic cells present in thymus and the primary function of which is the generation of T cells. Proliferation of splenocyte and thymocyte is an indicator of immunostimulation. Splenocyte and thymocyte proliferation in the presence of PS-I was used to evaluate cell stimulatory effects on the immune cell activation. Both the splenocyte and thymocyte proliferation indices were found maximum at 50 µg/mL, above and below which it decreases. Hence, it can be concluded that 50 µg/mL is the optimum concentration of the PS-I for splenocyte and thymocyte proliferation.

CHAPTER-V: A green synthesis of gold nanoparticles (Au NPs) using aqueous solution of a hetero polysaccharide, extracted from the gum of *Cochlospermum religiosum* (katira gum), has been demonstrated in this chapter. Here, the hetero polysaccharide plays the role of both reducing and stabilizing agent.

Synthesis and characterization of Au NPs

For the synthesis of Au NPs, 2 mL aqueous solution of chloroauric acid ($HAuCl_4$) with a concentration of 10^{-3} M was added to 6 mL 0.2 % (w/v) aqueous polysaccharide solution. The mixture was then heated at 70 °C for 6 h with continuous stirring on a magnetic stirrer and UV-vis spectra of the reaction mixture were recorded at different time interval till the completion of the reaction. A pale pink color was appeared after 10 min of the reaction and the color was gradually intensified as the reaction was continued with heating. A typical plasmon resonance band at 544 nm appeared after 1 h indicating formation of Au NPs. The intensity of the absorption band gradually increased and the maximum intensity of absorption was attained after 6 h of the reaction. This gradual increase in the absorption band is attributed to the fact that Au NPs concentration increases in the media as the reduction reaction proceeds. After 6 h, no significant change in intensity at 528 nm was observed which indicated almost complete reduction of Au^{+3}. The shifting of surface plasmon absorption maxima from 544 nm to a fixed value 528 nm at 6 h may be due to decrease in particles size.

The shape, morphology, and size distribution of the Au NPs were analyzed using high resolution transmission electron microscopy (HR-TEM). HR-TEM image showed that the

particles are mostly spherical with a few having rod and decahedral morphology. The average size of the particles is 6.9 nm as revealed from particle size distribution histogram. The SAED pattern showing rings ascribed to (111), (200), (220), (311), and (331) planes exhibited the face centered cubic (fcc) crystalline structure of gold. The crystalline nature of Au NPs was further confirmed by X-ray diffraction (XRD) analysis. A typical XRD pattern exhibited peaks at 38.22º, 44.40º, 64.51º, and 77.49º that can be indexed to the (111), (200), (220), and (311) facets, respectively of fcc gold. In order to investigate the interaction of Au NPs with the polysaccharide, FT-IR experiment of both the polysaccharide and Au NPs-polysaccharide bioconjugates were carried out. In the FT-IR spectrum of polysaccharide, two partially overlapped peaks at 1071 and 1043 cm^{-1} were assigned to C-OH stretching along with a broad stretching peak at 3428 cm^{-1} for hydroxyl group and a weak band at 2935 cm^{-1} for aliphatic C-H stretching. In the FT-IR spectrum of Au NPs-polysaccharide bioconjugates two overlapped peak at 1071 and 1043 cm^{-1} merged to give a single peak at 1044 cm^{-1}, which is possibly due to the interaction of Au^{+3} with the oxygen of hydroxyl group (C-OH) from polysaccharide. The peaks for hydroxyl group (3400 cm^{-1}), aliphatic C-H (2924 cm^{-1}) and C-OH (1044 cm^{-1}) are also appeared in the spectrum of Au NPs-polysaccharide bioconjugates which are the characteristic peaks of polysaccharides. So, it can be believed that there is some interaction between the Au NPs and polysaccharide with the help of which the Au NPs attain stability.

Catalytic activity of Au NPs-polysaccharide bioconjugates

To investigate the catalytic activity of Au NPs-polysaccharide bioconjugates, the reduction of 4-nitrophenol (4-NP) to 4-aminophenol (4-AP) by $NaBH_4$ in aqueous phase was chosen as a model reaction. The absorption peak of 4-NP was red shifted from 317 to 400 nm immediately after the addition of $NaBH_4$ solution, which also associated with a color change of 4-NP solution from yellow to yellow green due to formation of 4-aminophenolate ion in alkaline condition. The absorption peak at 400 nm remained unaltered for a long duration in absence of Au NPs-polysaccharide bioconjugates. In contrast, with the addition of Au NPs-polysaccharide bioconjugates, the absorption peak height at 400 nm successively decreased with a concomitant appearance of two new absorption peaks around 230 and 300 nm with time, which was because of the generation of 4-AP. The blank experiment by adding only the hetero polysaccharide into the aqueous solution of 4-NP and $NaBH_4$ mixture, did not change the color or absorption peak of 4-nitrophenolate ions for more than 24 h, which clearly demonstrated that the reduction of 4-

NP by $NaBH_4$ is solely activated by Au NPs-polysaccharide bioconjugates. The formation of 4-AP in the catalytic reaction was further confirmed by the ^1H NMR study in D_6-DMSO. As the initial concentration of $NaBH_4$ largely greater than the initial concentration of 4-NP, it can be assumed that concentration of $NaBH_4$ remains constant with time during the reaction. Hence, the reaction rate is independent on the concentration of $NaBH_4$. So pseudo-first-order rate kinetics with respect to 4-NP concentration was used to evaluate the rate of the reaction and reaction rate constant is determined to be 2.67×10^{-2} min^{-1}.